Mathematical Modelling To Predict Bead Geometry And Shape Relationship Of MIG Welded Aluminium 1200 Plates

Loveleen Gautam[1], Sahil Hanfi[2], Aayush Yadav[3], Dr. Pradeep Khanna[4]

[1,2,3]Student, MPA Engineering Division, NSUT New Delhi
[4]Associate Professor, MPA Engineering Division, NSUT New Delhi

---

Abstract- *Metal Inert Gas (MIG) welding is a widely used joining process across the industry. It uses a solid consumable filler wire which is heated and melted by generating an arc between wire and the workpiece. The popularity of this welding technique is because of its versatility, high quality welds, ability to get fully automated and use in mass producing units. The process can successfully weld a large number of materials for which suitable filler wire can be made available. Aluminium is a material of immense industrial potential because of its many favourable mechanical properties. It poses a little reluctance towards joining through welding. The present work involves investigating the weldability of aluminium from the view point of weld bead geometry and shape relationship. Aluminium grade 1200 has been selected for the present work because of its utility in manufacturing pipelines, shipbuilding industry, etc. the important input parameters chosen for the study were welding speed (WS), voltage and wire feed rate (WFR). An attempt is made to establish a mathematical relationship between the input and response parameters which in this case are weld width (W), height of reinforcement (HOR) and weld reinforcement form factor (WRFF), which is the ratio of W and HOR. Design of experiment (DoE) technique was used to conduct the experiments in a structured way and develop the model, response surface methodology is used to analyse the results graphically. The developed model was analysed and its significance was checked using ANOVA analysis.*

Key Words: MIG, aluminium, input welding parameters, mathematical model, ANOVA analysis

1.0 INTRODUCTION

MIG welding has its widespread applications in automotive industry, pipeline welding, shipbuilding industry and many more because of its ability to produce uniform, slag-free, clean and strong welds. Welding of aluminium is a little difficult process because of two main reasons; first being the formation of refractory oxide layer on its surface and second is its high thermal conductivity. The oxide layer is refractory in nature with very high melting point. This oxide layer poses difficulties during the welding of aluminium. The oxide layer acts as an insulator resulting in difficulty in establishment of arc between the work and the electrode. Secondly, the high conductivity does not allow the heat of welding to raise local temperature to rise to the melting point thereby resulting in no welding. Special steps are required to be taken for the welding of this metal.

Typical steel liners can scratch and shave aluminium feed wire easily being hard inside. Teflon liners were used in place of steel liners to reduce friction and eliminate wire shaving. burnback is also very common in MIG welding of aluminium. To prevent burnback, nozzle plate distance was increased and copper-zirconium alloy contact tips were used along with increasing the shielding gas flow rate. Researchers have made various attempts to predict and interpret the effects of welding parameters on the weld bead [1-4]. The intricacy of the weld bead is directly affected by weld schedules and thus the manufacturing costs of assemblies and procedures [5]. The welded joints have been found to fracture from the weld deposit, close to fusion line. This is because of presence of porosity in this area [6]. Instead of many challenges faced during the welding of aluminium, the material still offers many lucrative advantages as a construction material, being its easy workability, machinability and excellent strength to weight ratio. In the present case, aluminium 1200 is used because of its high corrosion resistance, good weldability and high anodising capability. It also possesses high co-efficient of reflection and high thermal conductivity. It is classified as a non-heat treatable commercially pure aluminium inspite of 99% minimum requirement for aluminium content. Aluminium 1200 used consists of aluminium (minimum 99%), iron+silicon(1%), magnesium(0.05%), titanium(0.05%), manganese(0.05%), copper(0.05%), zinc(0.01%), and other elements(0.015%) [7].

DoE approach was used to generate the combination of experiments to be conducted. Central Composite Face centre design approach was found suitable for the number of variables and levels opted for the present study. This design comprises fractional factorial design with centre points, amplified using cluster of axial points (star points) that enables the correct approximation of the curvature. It is capable of predicting quite accurately the first order terms, second-order terms and interaction terms [8]. A total number of 15 runs were conducted. The software was used to develop the

mathematical model. The suitability of the developed model was verified by ANOVA technique. Response surface methodology was used to analyse the results graphically.

2.0 EXPERIMENTAL SET-UP

A constant voltage weld power source with flat V-I characteristics was used with rated capacity of 400 amp. A double roller wire feeder was used to supply filler wire to the weld pool without any slippage. The welds were conducted on a motor driven mechanised unit, which can facilitate the movement of the carriage at different steplessly controlled speeds ranging from 0-50cm/min. This not only ensures a consistent speed per weld run but also provides reproducible results which otherwise are impossible to achieve in manual welding. For this purpose, a variable frequency drive was used to control the electric motor from which the motion was transferred to the carriage through chain and sprocket mechanism. Industrial grade pure argon gas was used at 15 lpm for shielding purpose. Cu-Zr alloy contact tips were used so as to avoid the welding of filler wire with contact tip in the event of overheating. A specially developed straight head machine welding torch was attached to a radial rotating arm capable of moving up-down and across the table. A constant arc-length of 13 mm was maintained throughout the process.

Figure-1 Experimental setup

Figure-2 Wire feeder with carriage

3.0 PLAN OF INVESTIGATION

1. Identification of the input parameters and estimating their working ranges
2. Developing the design matrix
3. Conducting the experiments as per the design matrix
4. Specimen preparation and recording the responses
5. Developing the mathematical model
6. Testing the significance of the model
7. Results and their explanation
8. Conclusion

3.1 Identification of the input parameters and estimating their working ranges

A number of factors govern the resultant weld bead. Some of the factors are WFR, WS, voltage, torch angle and polarity. Trial runs were conducted in order to find out the workable parameters and their upper limits and lower limits. These parameters were decided keeping in view:

1. Appearance of welds
2. No spattering and undercuts
3. No burnout and visible cracks

The final input parameters and their working limits are listed in the table 1.

Table 1: Input parameters and their working ranges

Process parameters	-1	0	1
WFR (mm/min)	5	6	7
WS	40	45	50
Voltage (Volts)	16	18	20

3.2 Developing the design matrix

DoE was used to generate a matrix of three-factors three-levels using central composite face centred technique with a total of 15 runs.

Table 2: Design matrix

S.No.	Run	Factor 1 A:WFR (m/min)	Factor 2 B:WS (cm/min)	Factor 3 C:Voltage (volts)
7	1	0	-1	0
3	2	-1	1	1
9	3	0	0	-1
5	4	-1	0	0
10	5	0	0	1
14	6	0	0	0
13	7	0	0	0
11	8	0	0	0
2	9	1	-1	1
8	10	0	1	0
1	11	1	1	-1
6	12	1	0	0
12	13	0	0	0
4	14	-1	-1	-1
15	15	0	0	0

3.3 Conducting the experiments as per the design matrix

The experimental runs were performed by following the combinations of input parameters suggested in the design matrix. These runs were made in arbitrary order in order to keep any systematic error at bay.

3.4 Specimen preparation and recording the responses

After the welding process was completed, the workpiece's surface was ground to make the surface polished and suitable to take etching. After grinding and polishing, the edges were chemically treated by a process known as etching. Etching is a high precision subtractive process that uses chemical compounds that removes or degrades the metal layer by layer. This was done in order to make the welding penetration inside the workpiece visible enough to carry out further recordings. A photograph of an etched specimen is shown in figure 3.

Figure 3: Etched specimen

Figure-4 Profile projector

To measure the parameters of the bead profile, a standard practise of shadow graphy was used in which a profile projector (figure-4) model number OPTO-MET V-14 DR was used to project the reflected image of the bead at 10x magnification. The measurements were taken by moving the x-y slides and observations were recorded using a DRO unit with a resolution of 0.001 mm. the observed values for width and the HOR are given in table – 3, below.

Table 3: Observations

Std	Run	Factor 1 A:WFR m/min	Factor 2 B:Welding speed cm/min	Factor 3 C:Voltage Volts	Response 1 Width Of Bead mm	Response 2 Height Of Reinf... mm	Response 3 WRFF
7	1	6	40	18	8.372	3.163	2.646
3	2	5	50	20	6.353	1.71	3.715
9	3	6	45	16	5.269	3.595	1.465
5	4	5	45	18	7.835	2.55	3.072
10	5	6	45	20	8.649	2.292	3.773
14	6	6	45	18	7.779	2.704	2.876
13	7	6	45	18	7.844	2.245	3.493
11	8	6	45	18	7.461	2.26	3.301
2	9	7	40	20	9.782	3.683	2.655
8	10	6	50	18	6.878	3.074	2.237
1	11	7	50	16	7.091	4.444	1.595
6	12	7	45	18	9.527	2.921	3.261
12	13	6	45	18	7.13	2.691	2.649
4	14	5	40	16	4.634	4.239	1.093
15	15	6	45	18	6.95	2.974	2.336

3.5 Developing the mathematical model

The mathematical equation developed by the software expressing the direct interaction and quadratic relations of the input parameters with the responses are given below:

$W = 7.66 + 0.8460*A - 0.7470*B + 1.69*C + 0.5875*AB - 0.5040*AC - 0.6255*BC + 0.7419*A^2 - 0.3141*B^2 - 0.9801*C^2$

$HOR = 2.60 = 0.1855*A - 0.0445*B - 0.6515*C + 0.1710*AB + 0.3975*AC - 0.3590*BC + 0.1152*A^2 + 0.4982*B^2 + 0.3232*C^2$

$WRFF = 2.95 + 0.0945*A - 0.2045*A + 1.15*C + 0.2335*AB - 0.5950*AC + 0.2340*BC + 0.2000*A^2 - 0.5250*B^2 - 0.3475*C^2$

3.6 Testing the significance of the model

The developed models were tested by the analysis of various techniques. The brief summary of outcomes is given below:

Table-4: ANOVA results

S No.	Response	Sum of Squares	df	Mean Square	F-Value	P-Value	R^2	Significant or Not
1	W	25.73	9	2.86	10.06	0.0102	0.9476	Yes
2	HOR	7.73	9	0.8590	10.63	0.0090	0.9503	Yes
3	WRFF	8.44	9	0.9376	5.25	0.0413	0.9043	Yes

From table 4, it is clear that the developed models are significant. The scatter diagrams given in figures 5 to 7 also show a close and non-random distribution of predicted versus actual values around the central line, further confirming the adequacy of the developed models.

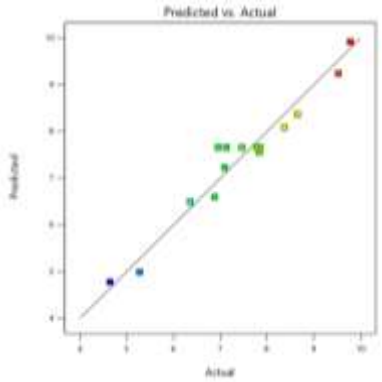

Figure-5 W

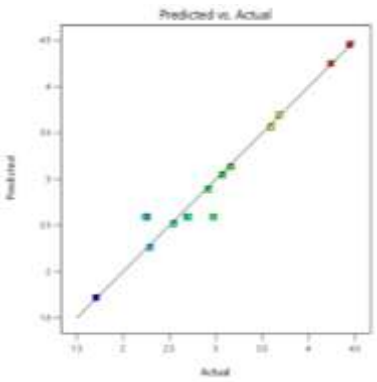

Figure-6 HOR

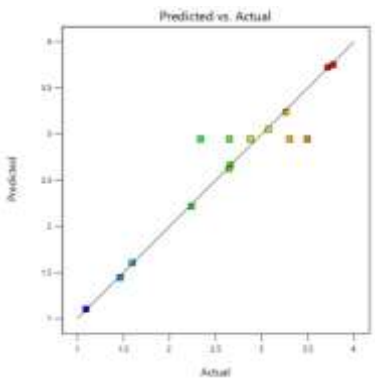

Figure-7 WRFF

3.7 Results and their study

The graphical results obtained from the software are given from figure 8-17. These results are indicating the effects of input parameters on various responses and can be divided into two categories - direct effects and interaction effects of input parameters on various responses.

3.7.1 Directs effects of input parameters on various responses

The directs effects of input parameters that is WFR, WS and voltage on response parameters which are W, HOR and WRFF are given in figures 8-10.

3.7.1.1 Direct effects on W

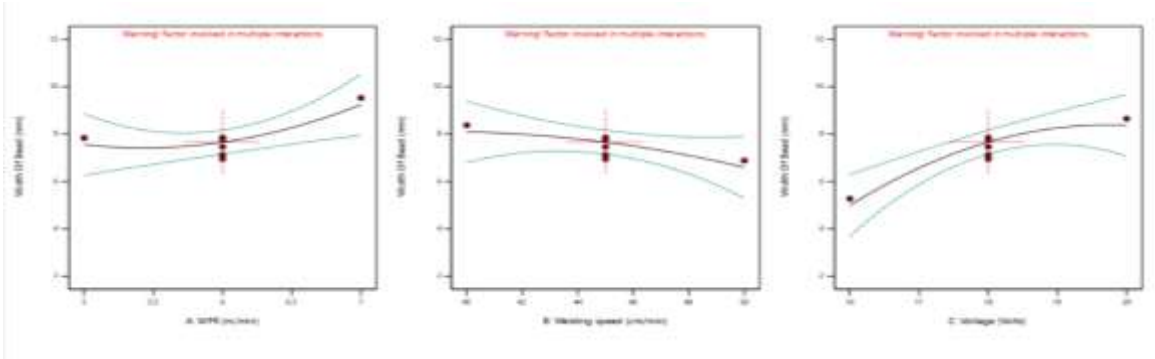

Figure 8- Direct effects on W

From figure 8, it is easy to conclude that WFR has positive, WS has negative and voltage has strong positive effect on W. The probable reasons for these trends could be that with the increase in WFR, the amount of weld current also increases resulting in more melting of filler metal which then has a tendency to spread over a large area causing increase in width. With the increase in WS, the heat input per unit weld decreases and less time is available for the filler wire to mix with base metal resulting in lesser spread of filler on the base metal surface. Voltage has a strong positive effect on W, the reason could be attributed the fact that with increase in voltage, the overall arc energy increases and the weld bead redistributes itself because of more spread of the arc with the increase in voltage resulting in a wider bead.

3.7.1.2 Direct effects on HOR

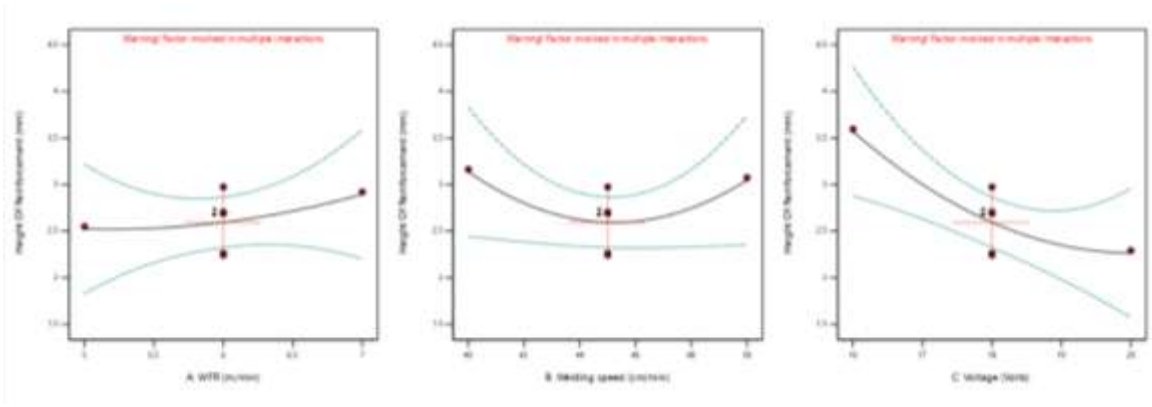

Figure 9- Direct effects on HOR

From figure 9, it can be concluded that WFR has slightly positive, WS has initially negative, then positive and voltage has strong negative effect on the HOR. The probable reasons for these trends could be that with the increase in WFR as the amount of weld current also increases it results in more melting of filler metal which in turn causes an increase in the HOR. With the initial increase of WS, height decreases. The reason could be that at slow speeds the weld metal has tendency to penetrate more with resulting decrease in height. After a certain value of speed, the trend reverses because now the metal does not get opportunity to enter the weld, rather it simply sits on the base plate resulting in the increase in the HOR. Increase in the voltage has strong negative effect on the HOR, as mentioned previously that increase in voltage results in a wider spread arc resulting in further spreading of the molten metal causing decrease in the HOR.

3.7.1.3 Direct effects on WRFF

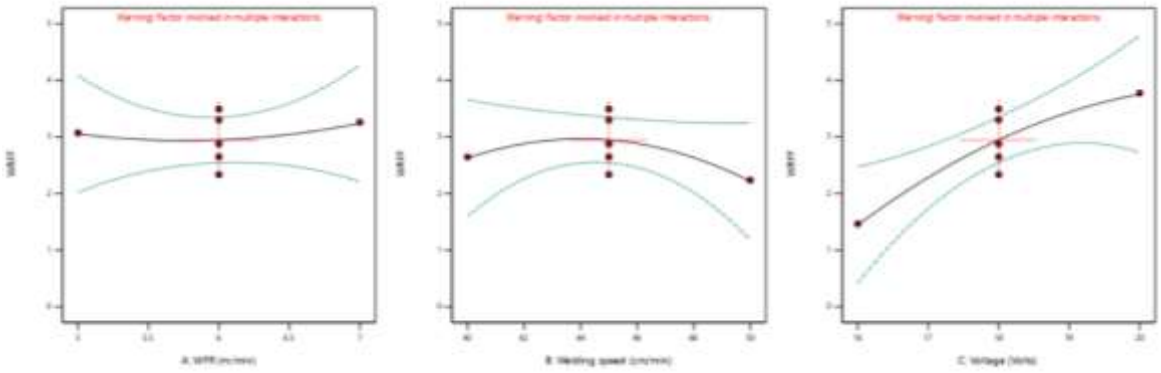

Figure 10- Direct effects on WRFF

From figure 10, it is easy to conclude that WFR has a slight positive, WS has an initial positive and then negative, and voltage has strong positive effect on WRFF. The probable reasons for these trends could be that with the increase in WFR, the W increases slightly more in comparison to HOR therefore leading to a slight increase in WRFF with increase in WFR. With the increase in WS, the W reduces with sharp reduction in HOR leading to positive effect in WRFF till mid-point of the graph. On further increase in WS, the W keeps on decreasing while HOR starts increasing giving a negative effect on WRFF. Voltage has a strong positive effect on WRFF, the reason is that with increase in voltage, the W has a sharp positive effect while HOR has a sharp negative effect. Therefore, the WRFF increases sharply on increasing voltage.

3.7.2 Interaction effects of input parameters on responses

The input parameters are set to have an interactive effect if by changing the level one parameter, the values of another parameter do not remain the same. Under such circumstances, the lines denoting both these parameters are no longer parallel. The interaction effects of various input parameters on response variables are explained in the following heading.

3.7.2.1 Interaction effects of WS and WFR on W

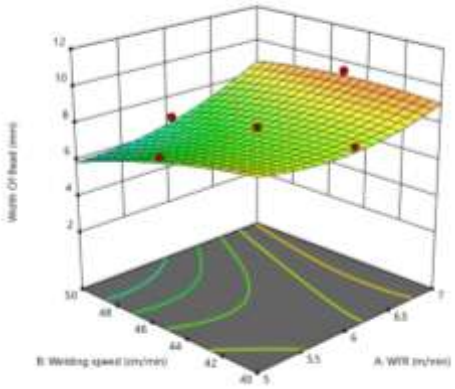

Figure 11: Interaction effects of WS and WFR on W

Figure 11 indicates the interaction effects of WS and WFR on width. It is evident that for all values of WFR, the width decreased with the increase in WS. The reason could be that with the increase in speed, there is less time available for the filler metal to spread resulting in thin and ropey bead. On the other hand, for all values of WS there is increase in W with the increase of WFR. The reason could be that with the increase of WFR, the welding current increased causing more melting of base metal and filler wire resulting in a wider bead.

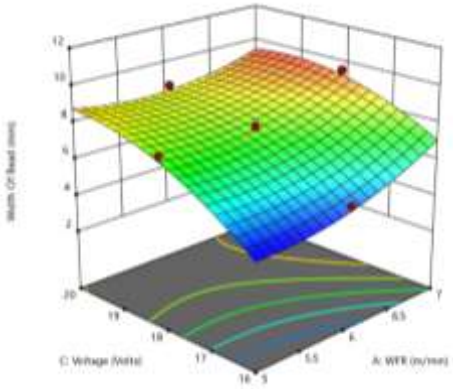

Figure 12: Interaction effects of WFR and voltage on W

Figure 12 shows the interaction effects of WFR and voltage on W. It is clear from the graph that for all values of WFR, the W increases with increase in voltage. The reason could be that with increase in voltage the overall arc energy increases causing more filler wire to melt and redistributed it over larger area due to increase in arc length causing wider arc spread. On the other hand, for major values of voltage the W increases with increase in WFR. Possible reason for this could be that with increase in WFR, current increases causing more melting of filler wire resulting in wide weld pool and wide W.

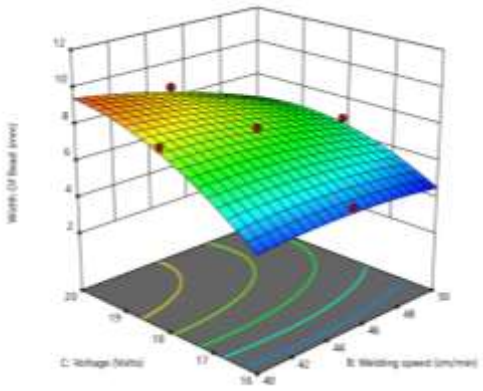

Figure 13: Interaction effects of WS and voltage on W

Figure 13 shows the interaction effects of WS and voltage on W. It is clear from the graph that for all values of WS, the W increases with increase in voltage. The possible reason could be that with increase in voltage, the overall arc energy increases and W redistributes itself because of wider arc spread causing wider W. On the other hand, for all values of voltages, the W decreases with increase in WS. The possible reason could be that with increase in WS the heat input per unit weld decreases and less time is available for filler metal to mix with base metal causing lesser spread of weld bead

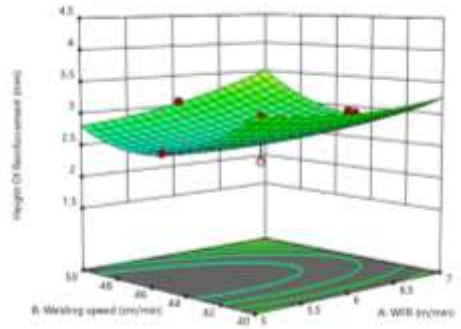

Figure 14: Interaction effects of WFR and WS on HOR

Figure 14 shows the interaction effects of WFR and WS on HOR. It is clear from the graph that for all values of WS the HOR increases with increase in WFR. The possible reason could be that with increase in WFR the weld current increases leading to more melting of filler wire resulting in increase in HOR. On the other hand, for all values of WFR, the HOR initially decreases with increase in WS but then starts increasing. The possible reason can be that at low speeds, the molten metal gets more time to penetrate resulting in decrease in HOR. But after a certain point, the trend reverses because now molten filler metal does not get enough time to penetrate, resulting in cooling on the upper surface and an increase in HOR.

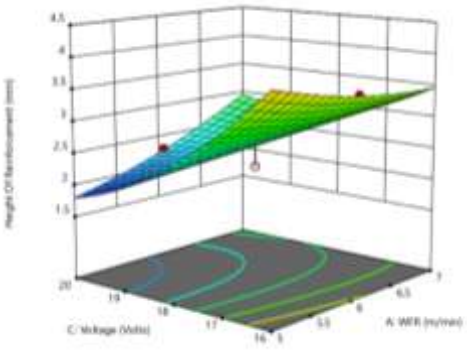

Figure 15: Interaction effects of WFR and voltage on HOR

Figure 15 shows the interaction effects of WFR and voltage on HOR. It is clear from the graph that for all values of WFR, the height decreases with increase in voltage. Possible reason for that could be that with increase in voltage the overall arc energy increases causing increase in arc spread resulting in wider spread of molten filler wire leading to a decrease in HOR. On the other hand, for all values of voltages the HOR increases with increase in WFR. The possible reason could be that with increase in WFR weld current increases leading to more melting of filler wire resulting in increase in HOR.

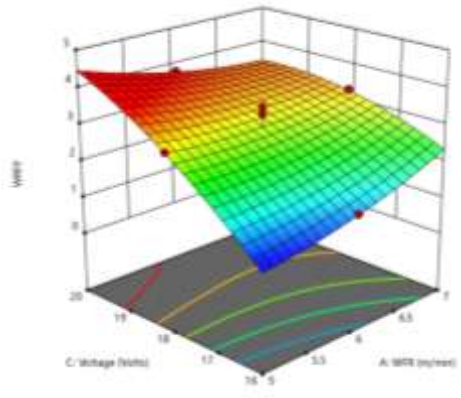

Figure 16: Interaction effects of WFR and voltage on WRFF

Figure 16 shows the interaction effects of WFR and voltage on WRFF. It is clear from the graph that for all values of WFR, the WRFF increases with increase in voltage. Possible reason for that is with increase in voltage, the W increases while the HOR decreases, resulting in increase in WRFF. On the other hand, at lower voltage, WRFF increases with increase in WFR. Reason for that is at lower voltage, W increases due to increase in current while HOR decreases with increase in WFR. But at higher voltage, the trend reverses. Reason for that is at higher voltage the W increased but at the same time the increase in height due to higher welding currents is more as compared to increase in width.

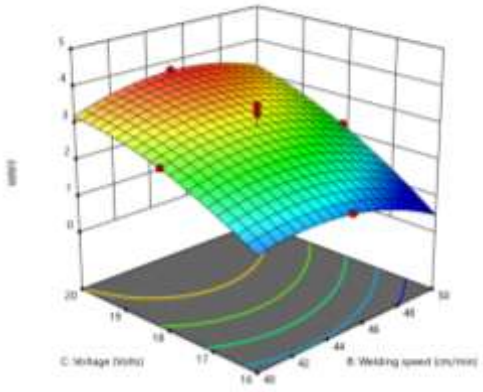

Figure 17: Interaction effects of voltage and WS on WRFF

Figure 17 shows interaction effect of voltage and WS on WRFF. It is clear from the graph that for all values of WS, the WRFF increases with increase in voltage. Possible reason for that is with increase in voltage, the W increases while HOR decreases resulting in overall increase in WRFF. On the other hand, for all values of voltage, the value of WRFF first increases up to a certain point and then decreases with increase in WS. Reason for that is with increase in WS up to certain limit, the W increases more pronouncing as compared to height. After this point the WRFF decreases with increase in WS. Reason for that is with further increase in WS the weld with starts decreasing while the HOR increases resulting in overall decrease in WRFF.

3.8 Conclusions

Following conclusions can be drawn on the basis of the work carried out so far:

1. The application of the technique of CCFD has been proved to be satisfactory.

2. The W was found to increase with the increase in voltage and WFR, whereas it reduced with the increase in WS.

3. The HOR was found to first decrease to a certain point and then increased with increase in WS, whereas it increased with the increase in WFR and decreased with the increase in voltage.

4. The WRFF was found to increase to a certain point and then decrease with increase in WS, while it increased with the increase in both WFR and voltage.

REFERENCES

[1] Optimization of weld bead geometry in MIG welding process using response surface methodology, Vol. 2 Issue 4, September 2012

[2] Investigation of Process Parameters during MIG Welding of AISI1010 Mild Steel Plates, IRJET Volume: 04 Issue: 04 | Apr -2017

[3] Effect on width, height and penetration of V-groove butt joint weld bead by varying process parameters, IRJET, Volume: 04 Issue: 12 | Dec-2017

[4] A Review on Parametric Optimization of MIG Welding by Taguchi's Method, IRJET,

Volume: 06 Issue: 10 | Oct 2019

[5]. K.N. Braszczy, nska-Malika, M. Mróz" Gas-tungsten arc welding of AZ91 magnesium alloy" Journal of Alloys and Compoundsc(2011).

[6] ranjan R., Kumar A – "Effect of Welding parameters on bead geometry of weld by GMAW Process", 2016 IJEDR | Volume 4, Issue 1 | ISSN: 2321-9939.

[7] Smiths Metal Centres 2018 - 1200 Aluminium Technical Datasheet

[8] 2019 Minitab, LLC - response surface designs, central composite designs, and Box-Behnken designs

BIOGRAPHIES

Loveleen Gautam is pursuing third year of her bachelor's degree in Manufacturing Processes & Automation Engineering

Sahil Hanfi is pursuing third year of his bachelor's degree in Manufacturing Processes & Automation Engineering

Aayush Yadav is pursuing third year of his bachelor's degree in Manufacturing Processes & Automation Engineering.

Dr. Pradeep Khanna is an Associate professor in the department of Manufacturing Processes & Automation Engineering.